Journal of Orthopaedic Translation 22 (2020) 50–57

Contents lists available at ScienceDirect

Journal of Orthopaedic Translation

journal homepage: www.journals.elsevier.com/journal-of-orthopaedic-translation

Original Article

Different subchondral trabecular bone microstructure and biomechanical properties between developmental dysplasia of the hip and primary osteoarthritis

Linyang Chu [a,☆], Zihao He [a,☆], Xinhua Qu [b], Xuqiang Liu [c], Weituo Zhang [d], Shuo Zhang [d], Xuequan Han [a], Mengning Yan [a], Qi Xu [a], Shuhong Zhang [a], Xifu Shang [e], Zhifeng Yu [a,*]

[a] Shanghai Key Laboratory of Orthopedic Implants, Department of Orthopedic Surgery, Shanghai Ninth People's Hospital, Shanghai Jiao Tong University School of Medicine, Shanghai, PR China
[b] Department of Bone and Joint Surgery, Renji Hospital, Shanghai Jiaotong University School of Medicine, Shanghai, 200011, PR China
[c] Department of Orthopedics, The First Affiliated Hospital of Nanchang University, The Artificial Joint Engineering and Technology Research Center of Jiangxi Province, Nanchang, PR China
[d] Clinical Research Center, Shanghai Jiao Tong University School of Medicine, Shanghai, 200025, PR China
[e] Department of Orthopedics, The Affiliated Provincial Hospital of China Science and Technology University, Hefei, 230001, Anhui Province, PR China

ARTICLE INFO

Keywords:
Biomechanical properties
Cartilage damage
DDH
Individual trabecula segmentation
Subchondral trabecular bone

ABSTRACT

Objective: Developmental dysplasia of the hip (DDH) is recognized as a frequent cause of secondary osteoarthritis (OA). The purpose in this study was to compare structural and biomechanical properties of subchondral trabecular bone and its relationship with cartilage damage between patients with DDH and patients with primary hip OA.
Methods: Forty-three femoral head specimens obtained from patients who underwent total hip arthroplasty [DDH, n = 17; primary OA, n = 16; and normal control (NC), n = 10] were scanned by microcomputed tomography and analyzed by individual trabecula segmentation to obtain the microstructural types of subchondral trabecular bone. The biomechanical properties were analyzed by micro–finite element analysis, and cartilage damage was evaluated by histology. The linear regression analysis was used to indicate the association between microstructures, biomechanical property, and articular cartilage.
Results: The DDH group showed the lowest total bone volume fractions (BV/TV) and plate BV/TV in the three groups ($p < 0.05$). There were also different discrepancies between the three groups in plate/rod trabecular number, plate/rod trabecular thickness, trabecular plate surface area/trabecular rod length, and junction density with different modes (plate–plate, rod–rod, and plate–rod junction density). The micro–finite element analysis, histology, and linear regression revealed that the subchondral trabecular bone in the DDH group had inferior biomechanical properties and cartilage damage of patients with DDH was more serious with different subchondral trabecular bone microstructures.
Conclusion: Our findings detected deteriorating subchondral trabecular bone microstructures in patients with DDH. The mass and type of subchondral trabecular bone play a key role in mechanical properties in DDH, which might be related to cartilage damage.
The translational potential of this article: Our findings suggested that changes of subchondral trabecular bone play a critical role in DDH progression and that the improvement on subchondral trabecular bone may be a sensitive and promising way in treatment of DDH.

Introduction

Developmental dysplasia of the hip (DDH) is a disabling musculoskeletal disease that impairs the developing hip joint [1]. DDH is an anatomic deformity resulting in inhomogeneous stress distribution and secondary osteoarthritis (OA) because it changes the gross morphology of the joint structure [2]. Based on a cross-sectional survey, DDH affects a high proportion (1.52%) of ageing adults in China; 20% of these patients

* Corresponding author. Shanghai Key Laboratory of Orthopedic Implants, Shanghai Ninth People's Hospital, 639 Zhizaoju Road, Shanghai, 200011, PR China.
E-mail address: zfyu@outlook.com (Z. Yu).
☆ These authors contributed equally.

https://doi.org/10.1016/j.jot.2019.09.001
Received 9 May 2019; Received in revised form 29 August 2019; Accepted 3 September 2019
Available online 27 September 2019

younger than 50 years have clinical indication for total hip arthroplasty (THA) [3]. Given its large population, China may bear the highest DDH-related burden compared with other countries. DDH has become a public health challenge, which underscores the need for urgent comprehensive therapy.

The radiographic measurements remain the primary basis for the diagnosis of DDH [4]. Patients with early-stage DDH definitively develop secondary OA, with 50% of these patients developing advanced OA at the age of 50 years [5]. Compared with primary hip OA, DDH often causes more severe symptoms and imaging manifestations (i.e., early hip instability and limited mobility, abnormal joint loading and stress distribution, absorption of the femoral head, and hip dislocation causing formation of a false joint) [6,7]. Some studies have illustrated changes in the subchondral trabecular bone microstructure in primary OA [8,9]. Although the characteristics of DDH are quite similar to those of primary OA, discrepancies in the subchondral trabecular bone microstructure between these conditions are largely unknown. Knowledge of these discrepancies may help optimise the surgery plan of DDH, and subchondral trabecular bone may be a target for the treatment of early-stage DDH.

Recently, imaging technologies, i.e., microcomputed tomography (micro-CT), have revealed key evidence indicating the imperative role of the subchondral microstructure in the pathogenesis of primary OA [8,10]. Meanwhile, micro–finite element analysis (μFEA) was used to quantitatively analyze the biomechanical properties and their relationship with the subchondral trabecular bone microstructure in patients with OA [11]. However, there are several limitations to the current standard morphological analysis. The individual trabecula segmentation (ITS) analysis maintaining essentially all the plate and rod microarchitecture, number, shape, volume of trabecular plates and rods, and connectivity between trabecular plates–plates, plates–rods, and rods–rods, can evaluate the detailed trabecular bone network [12]. Specifically, the morphological parameters might be insensitive to subtle variations in statistical means of the imaged bone trabecular network, compared with single measurement values of the individual trabecula [12]. In this study, our aim was to indicate the structural and mechanical property of subchondral trabecular bone and articular cartilage in patients with DDH. We explored the relationship among the subchondral trabecular bone microstructure, biomechanical properties, and cartilage damage. We hypothesized that the changes of the subchondral trabecular bone microstructure might be correlated with biomechanical properties and cartilage damage in patients with DDH.

Materials and methods

Specimen preparation

In this study, femoral head specimens were obtained from 17 patients with DDH (DDH group, 45.8–55.2 years) and 16 patients with primary hip OA (OA group, 50.1–68.4 years). All patients who underwent THA were diagnosed as having DDH or primary hip OA based on radiographic and clinical diagnostic criteria by an experienced surgeon in orthopaedic surgery at Shanghai Ninth People's Hospital [5,13]. Furthermore, 10 healthy femoral heads from patients with the fractured femoral neck who underwent THA in the same hospital constituted the normal control group (NC group, 48.4–61.3 years). This study was approved by the Institutional Review Board of Shanghai Ninth People's Hospital (IRB reference number: 2018-179-T137). All patients provided informed written consent before their participation in this study. All patients had a detailed history and physical examination, as well as biochemical marker detection tests, to exclude those with systemic diseases, such as haematological disorders, endocrine diseases, thyrotoxicosis, metabolic diseases of the liver and kidney, or malignancies that may have affected systemic bone metabolism. The femoral head specimens were refrigerated for follow-up studies.

Micro-CT scanning and ITS-based morphological analysis

All bone specimens were scanned using the high-resolution micro-CT system (Micro-CT 80; Scanco Medical AG, Switzerland) with 36-μm isotropic voxel size [14]. There are particular patterns of the trabecula, which correspond to the compressive and tensile region in the stressed central position of the femoral head [15]. The principal region that is perpendicular to articular surface is well suited for studying bony changes because it can respond to the transferred loading forces from the diseased articular surface [16,17]. Moreover, it has been shown that the cylinder axis of the principal load-bearing region is aligned with the main trabecular direction; thus, measured changes in biomechanical properties, taking into account the testing direction, can be minimized [17].

Based on the aforementioned theory, virtual cylindrical biopsies (Ø, 5.4 mm; L, 5.4 mm) determined by the semiautomatic contouring method as the volume of interest in the principal load-bearing region were extracted from the reconstructed 3D image 2 mm below the surface of subchondral bone (cubic subvolume, Fig. 1). All scanned

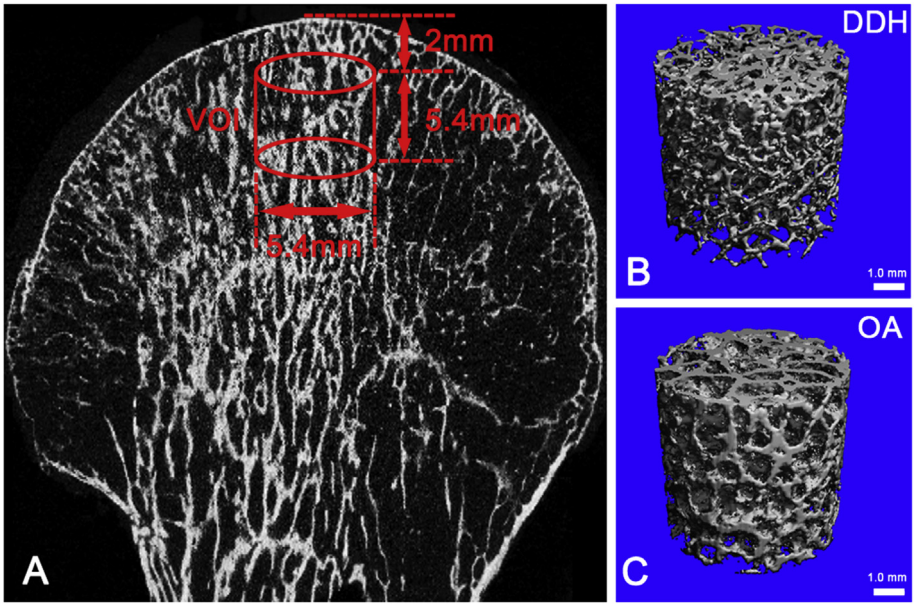

Figure 1. Micro-CT view of the femoral head specimens. (A) The location of virtual cylindrical biopsies extracted from the image (cubic subvolume of interest). (B–C) The reconstructed 3D image of the DDH and OA group. CT = computed tomography; DDH = developmental dysplasia of the hip; OA = osteoarthritis.

images were segmented by a low-pass filter to remove noise and then to determine the bone phase by the same threshold. The Micro-CT system software (Scanco Medical AG, Image Processing Language version 4.29d; Switzerland) was used to process the microstructural parameters. The total bone volume fraction (BV/TV), bone trabecular number (Tb.N), and bone trabecular thickness (Tb.Th) were obtained automatically. A model based on the type of the structure was used to measure the structure model index (SMI). An ideal segmented plate structural model has an SMI value of 0, whereas a segmented cylindrical rod structural model has an SMI value of 3. Meanwhile, connectivity density was defined to be a topological parameter of total bone trabecular connections per cubic millimetre.

ITS-based morphological analysis was applied for all bone trabecular cubic subvolumes in the DDH, OA, and NC groups. The bone trabecular network was resolved into individual plates and rods using a volumetric decomposition technique. In brief, with the digital topologic analysis, the skeletal network of the bone trabecular network was transformed into a representation skeleton made of surfaces and curves. Then, the plate and rod shapes of the subchondral microstructure were maintained. Each skeletal voxel was uniquely identified using the digital topologic analysis classification. Using the iterative reconstruction measure previously reported, each voxel was classified into an individual type of either the plate or rod [18]. Based on analysis of the separate bone trabecular plate or rod, a series of ITS-based morphological parameters were calculated at the junctions of both the plate and rod trabecula, i.e., plate and rod bone trabecular volume fraction (pBV/TV and rBV/TV), axial bone trabecular volume fraction along the longitudinal axis (aBV/TV), plate and rod tissue fraction (pBV/BV and rBV/BV), a ratio of trabecular plate versus rod (P/R ratio), plate and rod trabecular number density (pTb.N and rTb.N), plate and rod trabecular thickness (pTb.Th and rTb.Th), trabecular plate surface area (pTb.S), trabecular rod length (rTb.L), and plate–plate, plate–rod, and rod–rod junction density (P–P, P–R, and R–R Junc.D). The definition of these ITS-based microstructural parameters and detailed methods of applications were reported in the previous study [18].

Micro–finite element analysis

Scanco Medical Finite Element Software 1.06 (Scanco Medical AG, Switzerland) was used for μFEA to simulate the axial compression tests for each trabecular bone cube in the longitudinal directions. Micro-CT images were converted into 3–4 million micro–finite element models to represent hard tissue (36 μm/voxel) with eight-node brick finite elements. Bone material properties at the tissue level were assumed to be homogeneous linear isotropic material with an isotropic linear elastic material with a Young's modulus (Es) of 15 GPa and a Poisson's ratio of 0.3 [19,20]. For the bone segment model, uniaxial compression tests were used for μFEA analysis to compute the reaction force under a displacement equal to 1% of bone segment height along the axial direction. Bone stiffness and failure load were the mechanical parameters extracted from the FEA.

Histological analysis

After micro-CT scanning, specimens of the DDH, OA, and NC groups corresponding to the volume of interest were processed for cartilage evaluation through the histological analysis. In brief, serial sections (5 μm) were stained using haemotoxylin and eosin, Safranin O-Fast Green, and toluidine blue. Cartilage damage was assessed using the Osteoarthritis Research Society International (OARSI) scoring system in the three groups [21]. Five sections from each sample were stained and measured.

Statistical analysis

All values are expressed as means ± standard deviations. Independent two-sided Student t tests and one-way analysis of variance were used to test for significant differences in the ITS-based microstructural parameters and biomechanical properties between the DDH, OA, and NC groups. Pearson correlation coefficients were calculated for ITS-based microstructural parameters with each potential covariate. Sets of covariates with $p < 0.05$ and independent from each other were selected. These included age, height, and Harris Hip Scores. The ITS-based microstructural parameters were compared again after adjusting for the selected covariates by a generalized multiple linear analysis. To indicate the relationship between the microstructure, biomechanical properties, and cartilage damage in the DDH, OA and NC groups, linear regression analyses were performed; a two-tailed $p < 0.05$ was considered statistically significant. The statistical analysis was performed using the SPSS 19.0 software package (SPSS Inc., Chicago, IL, USA).

Results

The study population consisted of 17 patients with DDH and 16 patients with primary hip OA, and 10 patients with the fractured femoral neck constituted the NC group. All patients had no other systemic diseases, such as haematological disorders or endocrine diseases. As shown in Table 1, compared with patients with DDH, those with OA underwent operative treatment at an older age ($p < 0.05$). However, patients with DDH and OA were not different in weight and body mass index, indicating that obesity was not an interference factor. The Harris Hip Scores showed no joint function and daily activity differences between the DDH and OA groups.

The means and standard deviations of the micro-CT, ITS-based microstructure analysis for the three groups and the percentage differences between the DDH and OA groups are presented in Table 2 and Fig. 2, respectively. The BV/TV of the OA group was 48.9% higher than that of the DDH group ($p < 0.05$). The values of the SMI showed significantly morphological differences in the bone trabecula between the DDH and OA groups ($p < 0.05$). The ITS-based microstructural analysis more particularly confirmed this result. The aBV/TV of the OA group was 62.3% higher than that of the DDH group ($p < 0.05$). The DDH group had an 84.5% lower pBV/TV and a 30.8% lower pBV/BV than the OA group ($p < 0.05$). There was no difference in rBV/TV between the DDH and OA groups; however, the OA group had an 82.2% higher P/R ratio than the DDH group ($p < 0.05$). The results of standard micro-CT also showed that Tb.N and Tb.Th were 25.2% and 46.8% lower, respectively, in the DDH group than in the OA group ($p < 0.05$). Interestingly, the differences may have been caused by the plate-like trabecula because pTb.N, pTb.Th, and pTb.S were 33.1%, 43.7%, and 39.7% higher in the OA group, respectively ($p < 0.05$), whereas rTb.N, rTb.Th, and rTb.L were not significantly different in the DDH and OA groups (−2.5%, 0.7%, and 0.8%, respectively; $p > 0.05$). In addition, the connection and

Table 1
Basic information of the DDH, OA, and NC groups.

Characteristics	DDH (mean ± SD)	OA (mean ± SD)	NC (mean ± SD)	*p*, DDH versus OA
N	17	16	10	
Sex (women/men)	11/6	9/7	6/4	
Age (years)	50.3 ± 3.6	57.7 ± 4.8	55.8 ± 6.4	0.03
Height (m)	1.61 ± 0.04	1.66 ± 0.05	1.63 ± 0.09	0.04
Weight (kg)	58.3 ± 9.2	60.4 ± 11.7	61.9 ± 7.2	0.65
BMI (kg/m^2)	21.7 ± 1.2	22.1 ± 1.5	22.9 ± 2.1	0.74
Harris Hip Score (HHS)	62.1 ± 4.8	63.2 ± 3.9	78.6 ± 5.9	0.48
Alcohol use (%)	23.5%	31.2%	20%	
Current smokers (%)	17.6%	25%	37.5%	
Other systemic diseases	No	No	No	

BMI = body mass index; DDH = developmental dysplasia of the hip; NC = normal control; OA = osteoarthritis; SD = standard deviation.

Table 2
The subchondral microstructure of the specimens on standard micro-CT scans and ITS-based scans in the DDH, OA, and NC groups.

Microstructure	DDH (mean ± SD)	OA (mean ± SD)	NC (mean ± SD)	*p*, DDH versus OA
Standard micro-CT				
BV/TV (%)	23.18 ± 7.14	34.48 ± 8.72	30.63 ± 5.07	0.006*
Conn. Dens. (1/mm^3)	8.63 ± 4.91	11.96 ± 6.77	10.23 ± 4.28	0.04*
SMI	1.71 ± 0.88	0.51 ± 0.92	0.76 ± 0.63	0.03*
Tb.N (1/mm)	2.02 ± 0.51	2.53 ± 0.62	2.48 ± 0.74	0.04*
Tb.Th (mm)	0.17 ± 0.02	0.25 ± 0.03	0.23 ± 0.05	0.02*
ITS-based micro-CT				
aBV/TV (%)	10.17 ± 3.72	16.48 ± 5.23	13.17 ± 4.21	0.01*
pBV/TV (%)	13.64 ± 7.16	25.13 ± 8.24	21.77 ± 6.08	0.01*
rBV/TV (%)	9.54 ± 3.12	9.35 ± 4.26	8.86 ± 3.46	0.42
pBV/BV (%)	56.2 ± 22.1	73.5 ± 15.2	71.1 ± 13.7	0.04*
rBV/BV (%)	43.8 ± 11.4	26.5 ± 8.7	28.9 ± 7.9	0.03*
P/R ratio	1.69 ± 0.34	3.08 ± 0.48	2.46 ± 0.53	0.001*
pTb.N (1/mm)	1.84 ± 0.33	2.45 ± 0.26	2.19 ± 0.47	0.001*
rTb.N (1/mm)	2.39 ± 0.45	2.33 ± 0.64	2.21 ± 0.52	0.63
pTb.Th (mm)	0.19 ± 0.03	0.27 ± 0.04	0.24 ± 0.06	0.01*
rTb.Th (mm)	0.13 ± 0.11	0.13 ± 0.08	0.12 ± 0.06	0.79
pTb.S (mm^2)	0.07 ± 0.02	0.11 ± 0.02	0.10 ± 0.03	0.03*
rTb.L (mm)	0.45 ± 0.02	0.45 ± 0.01	0.47 ± 0.04	0.88
P–P Junc.D (1/mm^3)	8.42 ± 3.35	13.46 ± 6.51	11.28 ± 5.19	0.01*
P–R Junc.D (1/mm^3)	11.97 ± 3.92	18.26 ± 5.54	15.34 ± 5.28	0.008*
R–R Junc.D (1/mm^3)	7.47 ± 3.13	4.96 ± 2.28	4.77 ± 4.18	0.03*

*The *p*-value remained significant after adjusting for age, height, and Harris Hip Scores.
a = axial; BV = bone volume; Conn. Dens. = connectivity density; CT = computed tomography; DDH = developmental dysplasia of the hip; ITS = individual trabecula segmentation; NC = normal control; OA = osteoarthritis; p = plate; P–P Junc.D = plate-to-plate junction density; P–R Junc.D = plate-to-rod junction density; P/R ratio = plate-to-rod trabecular ratio; r = rod; R–R Junc.D = rod-to-rod junction density; SMI = structure model index; Tb.L = trabecular bone length; Tb.N = trabecular bone number; Tb.S = trabecular bone surface area; Tb.Th = trabecular bone thickness; TV = total volume.

junction densities (Conn. Dens., P–P Junc.D, P–R Junc.D, and R–R Junc.D) were the microstructural parameter that indicated the interlinking feature of the trabecular network. The Conn. Dens. was 38.4% higher in the OA group. Moreover, the P–P Junc.D and P–R Junc.D were 59.5% and 52.9% higher in the OA group, respectively ($p < 0.05$). However, the DDH group did show a greater R–R Junc.D than the OA group (−33.8%, $p < 0.05$). Furthermore, the generalized multiple linear analysis showed that all ITS-based data existed independently; adjustment for covariates (significant data in basic information) did not influence the significant differences in the microstructural variables between the DDH and OA groups (Table 2).

The results of the biomechanical properties determined on μFEA in the DDH, OA, and NC groups are shown in Fig. 3. The subchondral trabecular bone stiffness and failure load of the DDH group were significantly lower than those of the OA and NC groups. In addition, the analysis of linear regression was used to investigate the relationship between the major subchondral trabecular microstructure and biomechanical properties in the DDH, OA, and NC groups (Table 3). The results indicated that BV/TV and pBV/TV might be the key factors for biomechanical properties of subchondral trabecular bone in the three groups ($r^2 > 0.5$, Table 3). Moreover, the correlation coefficients for BV/TV and pBV/TV were higher in the OA group than in the DDH and NC groups, suggesting that subchondral trabecular bone in the OA group had greater biomechanical function than that in the DDH and NC groups when given the same amount of the total trabecula or plate trabecula. However, the microstructures of the rod trabecula were mainly negatively correlated with biomechanical properties in the DDH group, whereas there was no definite correlation in the OA and NC groups, suggesting that the rod trabecula partially influenced the biomechanical properties in patients with DDH, but not in patients with OA or normal people.

The histological results for cartilage evaluation were shown in Fig. 4A. Cartilage damage was obviously severer with cartilage surface destruction and proteoglycan disorder in the DDH group than in the OA group, and there was less cartilage damage in the NC group. The degenerative changes extended into the deep region in the DDH group. The assessment with the OARSI scoring system showed that the patients in the DDH group had worse cartilage condition than those in the OA and NC groups ($p < 0.05$, Fig. 4B). Meanwhile, the analysis of linear regression proved that BV/TV and pBV/TV were negatively correlated with cartilage damage in the combined data from the DDH, OA, and NC groups ($r^2 > 0.3$, Fig. 4C and D), whereas there was no definite correlation between rBV/TV and the OARSI score ($r^2 < 0.1$, Fig. 4E).

Discussion

In this study, we used the standard micro-CT, ITS morphological analyses, and the μFEA model to investigate the differences in the microstructural and biomechanical characteristics of subchondral bone between the DDH, OA, and NC groups. We found that the changes of the subchondral trabecular bone microstructure may have specific relationship with the biomechanical properties and cartilage damage in patients with DDH or primary OA.

In the trabecular segmentation technique, the subchondral trabecular bone can be resolved into rod-like or plate-like elements because there were microstructural differences between the two types [11,22]. It is increasingly evident that the types of trabecular bone (plate- or rod-like) play the crucial role in determination of trabecular biomechanical properties as rapid changes in these two types occur with disease progression [23,24]. ITS analysis basically contains the plate- and rod-related microstructures (i.e., the number, thickness, and bone volume of trabecular plates and rods), orientation, and connectivity between plate to plate, plate to rod, and rod to rod. By applying ITS-based micro-CT to decompose the subchondral trabecular bone microstructure, we observed differences in trabecular bone types between the DDH, OA, and NC groups that were not obvious in the conventional outcome measures [25]. The DDH group had lower bone volumes fraction, lower numbers of trabecular plates, thinner trabecular plates, and a lower trabecular P/R ratio than the OA and NC groups. However, rod bone volumes and rod trabecular numbers, thicknesses, and lengths were not obviously different between the three groups. These results provide insightful evidence that the plate-like trabecula holds the dominant position in patients with OA or normal people, whereas in patients with DDH, the plate trabecular bone may reduce gradually with disease onset and progression.

Prior studies have proved that trabecular plate number and thickness did not show obvious loss/reduction in a model of spontaneous OA [8,26]. However, in this study, we found that plate-like trabeculae in DDH were significantly fewer and thinner, and these changes may not affect the rod-like trabecula. DDH is a disabling musculoskeletal disease leading to secondary OA [27], but the reasons for the differing subchondral microstructure types between DDH and OA remain unknown. Some studies have reported that certain factors, i.e., osteoporosis, diabetes, and male vs. female sex, could cause changes in the subchondral trabecular bone microstructure [28–30]. We know that DDH is a congenital abnormality that definitely affects the development of hip joints in newborns [31]. Thus, the aetiology of the subchondral microstructure changes may be related to abnormal joint load and stress distribution, which is different from primary OA. In addition, in-depth examinations of rod–plate dynamics also revealed that patients with DDH had less connectivity between their plate–plate and plate–rod trabeculae, indicating a less connected and more widely separated trabecular network. We believe that the lower trabecular P/R ratio in DDH is the key reason

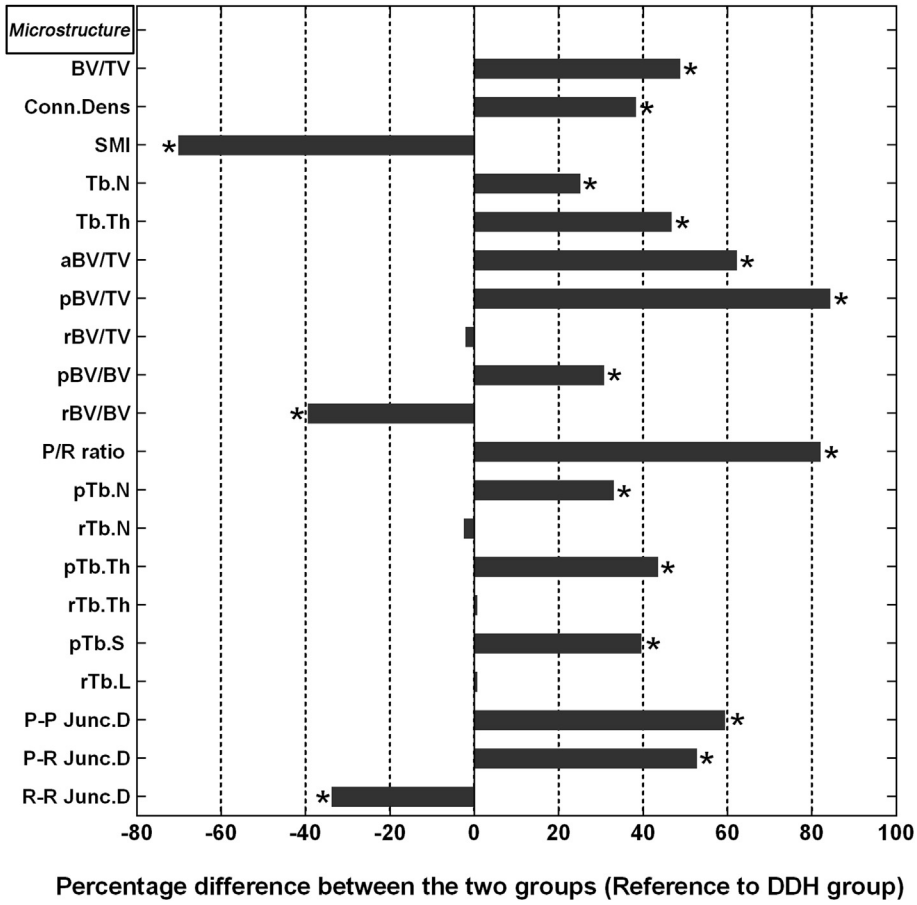

Figure 2. Percentage difference in the subchondral microstructures by ITS-based micro-CT analysis (OA group/DDH group). *Significant difference between the OA and DDH groups ($p < 0.05$). a = axial; BV = bone volume; Conn. Dens. = connectivity density; CT = computed tomography; DDH = developmental dysplasia of the hip; ITS = individual trabecula segmentation; OA = osteoarthritis; p = plate; P–P Junc.D = plate-to-plate junction density; P–R Junc.D = plate-to-rod junction density; P/R ratio = plate-to-rod trabecular ratio; r = rod; R–R Junc.D = rod-to-rod junction density; SMI = structure model index; Tb.L = trabecular bone length; Tb.N = trabecular bone number; Tb.S = trabecular bone surface area; Tb.Th = trabecular bone thickness; TV = total volume.

for deterioration of the microstructure and increased trabecular spacing and network inhomogeneity. Our results showed that the decreased trabecular P/R ratio in DDH is primarily due to a reduced number of plate-like trabeculae. Notably, patients with DDH have greater junction densities in rod–rod trabeculae than patients with OA, which suggests that the rod-like trabecula occupies an important position in the subchondral trabecular bone microstructure of the patient with DDH, which influences the interconnected bone trabecular network.

In the μFEA analysis, we further discovered that the biomechanical properties of subchondral trabecular bone (bone stiffness and failure load) were significantly lower in the DDH group than the in OA and NC groups, indicating that biomechanical function of subchondral trabecular bone in patients with DDH was severely compromised. Indeed, the subchondral trabecular bone microstructure is also an important determinant for biomechanics [32]. The microstructural types (plate- or rod-like trabecular bone) are independent and an essential factor that significantly correlates with the biomechanical properties [18]. In addition, the bone mass of the plate-like trabecula is more crucial to trabecular biomechanics than that of the rod-like trabecula. However, the existence of the latter is necessary for maintaining the integrity of the trabecular network and optimising the balance of the physiological environment [11,33,34]. In this study, linear regression showed that the changes of the plate trabecula may be positively correlated with the biomechanical properties in the DDH, OA, and NC groups, whereas the influence of the

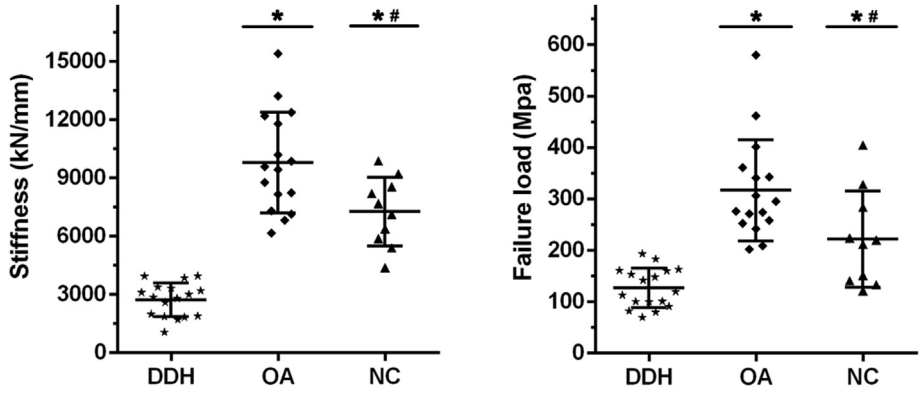

Figure 3. The biomechanical properties in the DDH, OA, and NC groups that are obtained by micro–finite element analysis (μFEA). *Significant difference compared with the DDH group ($p < 0.05$); #significant difference compared with the OA group. DDH = developmental dysplasia of the hip; NC = normal control; OA = osteoarthritis.

Table 3
Correlation coefficient of linear regression between the subchondral microstructure and biomechanical properties in the DDH, OA, and NC groups.

Microstructure	DDH		OA		NC	
	Stiffness	Failure load	Stiffness	Failure load	Stiffness	Failure load
BV/TV	0.54**	0.51**	0.88**	0.85**	0.63**	0.68**
Tb.N	0.23	0.21	0.46*	0.42*	0.37*	0.29
Tb.Th	0.37*	0.31*	0.71**	0.68**	0.55**	0.61**
pBV/TV	0.73**	0.66**	0.81**	0.82**	0.69**	0.71**
pTb.N	0.48*	0.43*	0.69**	0.65**	0.38*	0.41*
pTb.Th	0.33*	0.25	0.57**	0.41*	0.46*	0.39*
pTb.S	0.38*	0.28	0.59**	0.46*	0.51**	0.58**
rBV/TV	−0.39*	−0.41*	0.19	0.24	−0.13	0.08
rTb.N	−0.36*	−0.32*	0.21	0.23	0.14	0.17
rTb.Th	−0.32*	−0.24	0.11	0.16	−0.07	0.15
rTb.L	−0.22	−0.18	0.14	0.19	0.11	−0.12

*The p-value<0.05 indicated the significant correlation between the subchondral microstructure and biomechanical properties.
**The p-value<0.001 indicated the significant correlation between the subchondral microstructure and biomechanical properties.
BV = bone volume; Conn. Dens. = connectivity density; DDH = developmental dysplasia of the hip; NC = normal control; OA = osteoarthritis; p = plate; P–P Junc.D = plate-to-plate junction density; P–R Junc.D = plate-to-rod junction density; r = rod; R–R Junc.D = rod-to-rod junction density; Tb.L = trabecular bone length; Tb.N = trabecular bone number; Tb.S = trabecular bone surface area; Tb.Th = trabecular bone thickness; TV = total volume.

rod trabecula on biomechanical properties was relatively weak.

According to the correlation coefficient (the value of r^2) in the linear regression analyses, we deemed that the plate-like trabecula held a more essential role in patients with OA or normal people than in those with DDH. These results confirmed worsened biomechanical properties of subchondral trabecular bone in patients with DDH due to the different microstructures, although the clinical manifestations of the two diseases may be similar. Interestingly, in the DDH group, the rod-like trabecula was negatively correlated with biomechanical properties, whereas there was no definite correlation between rod-like trabeculae and biomechanical properties in the OA and NC groups. We speculated that as the extremely key function of the plate-like trabecula in stabilising the trabecular structure and withstanding joint load, the function of relatively fewer rod-like trabeculae on subchondral trabecular bone is not obvious. However, the rod trabecula occupies a certain percentage of bone in patients with DDH, which not only regulates the integrity of the trabecular bone network but also notably impairs biomechanical properties. Studies have proved that the subchondral trabecular bone changes may be accompanied with the entire primary OA development [8,35]. We considered that the synergistic effect of a decrease in the plate trabecula and an increase in the rod trabecula commonly leads to disease progression in patients with DDH.

We also demonstrated that the subchondral trabecular bone microstructural changes were associated with aggravated cartilage damage. Except for the rod-like trabecula, the total trabecula and plate-like trabecula were correlated with more severe cartilage destruction, which explained that secondary OA caused by DDH could exhibit more serious

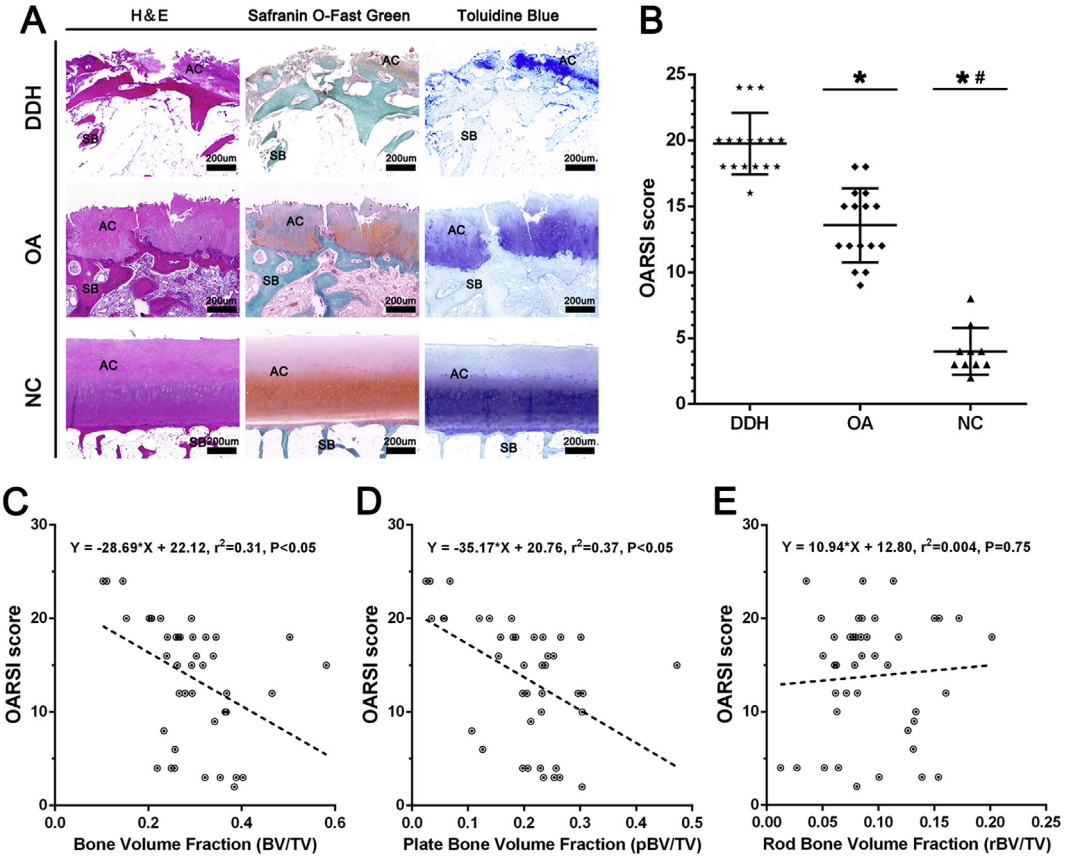

Figure 4. The articular cartilage evaluation and its association with the subchondral bone microstructure. (A) Histological analysis of cartilage damage in the DDH, OA, and NC groups. (B) The analytical results with the Osteoarthritis Research Society International (OARSI) scoring system. (C–E) Relationships between subchondral bone microstructure and cartilage damage. Data were combined from the DDH, OA, and NC groups. *Significant difference compared with the DDH group ($p < 0.05$); #significant difference compared with the OA group. AC = articular cartilage; BV = bone volume; DDH = developmental dysplasia of the hip; H&E = haemotoxylin and eosin; NC = normal control; OA = osteoarthritis; SB = subchondral bone; TV = total volume.

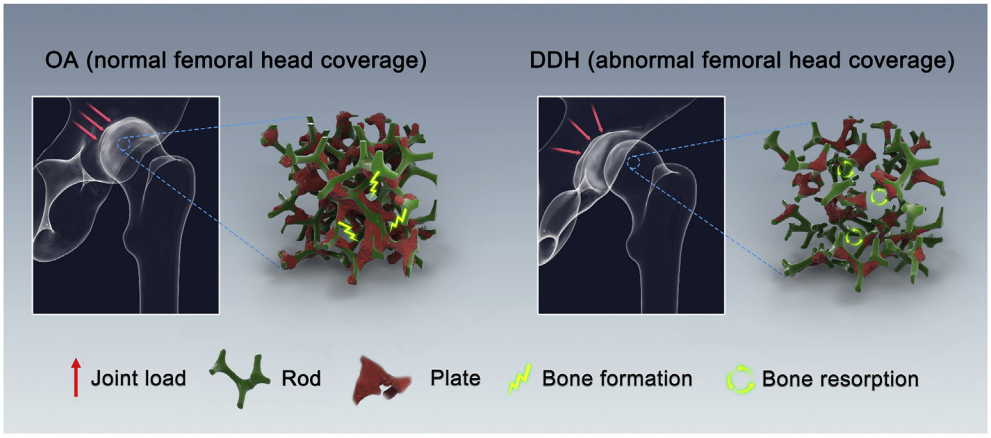

Figure 5. Schematic for the potential models of different subchondral microstructures between OA and DDH using the ITS-based micro-CT analysis. In OA, the subchondral bone mass would not decrease notably owing to the normal femoral head coverage and relatively uniform stress load. In DDH, the disorderly joint stress load caused by insufficient femoral head coverage could contribute to significant reductions in total trabecular volume and plate-like trabecula, which are harmful to the biomechanical properties and articular cartilage, thus resulting in accelerating the OA progression. CT = computed tomography; DDH = developmental dysplasia of the hip; ITS = individual trabecula segmentation; OA = osteoarthritis.

symptoms than primary OA (Fig. 5). The results suggested that subchondral trabecular bone changes in patients with DDH may play an important role in OA progression; this needs to be further confirmed by a prospective study.

Several limitations in our study should be mentioned. First, the results may be influenced by a selection bias because the study cohort comprised a relatively small sample of patients. However, the analysis between the microstructure and biomechanical properties in this study did not violate other research on other diseases, i.e., OA or osteoporosis [8,36,37]. Second, the analysis of the samples was based on femoral head specimens obtained from patients after THA. Ideally, the investigation should be based on *in vivo* assessments of the subchondral bone changes. Indeed, the XtremeCT is a promising and novel tool in clinical imaging that can provide visualisation of the trabecular microstructure *in vivo* [38]. At last, the study used the μFEA analysis [39]. The biomechanical properties identified from μFEA analysis reflect the effect of the microstructure but not the intrinsic mineral quality. It is unclear whether patients with DDH or OA were different in intrinsic bone characteristics, i.e., collagen and mineralization. We expect that these factors may be necessary to achieve in-depth understanding of the DDH pathogenesis.

Conclusion

In summary, we observed the characteristics in the microstructure and mechanical property of subchondral trabecular bone between patients with DDH and OA. More plate trabeculae were shown in OA, whereas more rod trabeculae were shown in DDH. Plate trabeculae may play a more important role in biomechanical properties of subchondral bone. The changes of subchondral bone may be related to the worsening biomechanical properties and severer cartilage damage, thus leading to the acceleration of OA progression in patients with DDH. Factors influencing the change of the plate and rod microstructure should be explored by future research.

Author contributions

L.C., X.S., and Z.Y. were involved in the design of the study, basic analysis of data, drafting of the manuscript, and revising it for critical knowledge content. L.C. and Z.H. performed the statistical analysis. X.Q., X.S., and X.L. were involved in the acquisition of data, drafting of the manuscript, and revising it critically for critical knowledge content. All authors have read and approved the final submitted manuscript.

Conflict of interest

The authors have no conflicts of interest to disclose in relation to this article.

Funding

This research was funded by the National Natural Science Foundation of China (no. 11572197, 11872251).

Acknowledgements

The authors thank the participated patients in this study. The authors also thank the participating surgeon who contributed by collecting data.

References

[1] Patel JH, Moed BR. Instability of the hip joint after posterior acetabular wall fracture: independent risk factors remain elusive. J Bone Joint Surg Am 2017;99:e126.
[2] Xu J, Li D, Ma RF, Barden B, Ding Y. Application of rapid prototyping pelvic model for patients with DDH to facilitate arthroplasty planning: a pilot study. J Arthroplast 2015;30:1963–70.
[3] Tian FD, Zhao DW, Wang W, Guo L, Tian SM, Feng A, et al. Prevalence of developmental dysplasia of the hip in Chinese adults: a cross-sectional survey. Chin Med J 2017;130:1261–8.
[4] Chadayammuri V, Garabekyan T, Jesse MK, Pascual-Garrido C, Strickland C, Milligan K, et al. Measurement of lateral acetabular coverage: a comparison between CT and plain radiography. J Hip Preserv Surg 2015;2:392–400.
[5] Kennedy JW, Brydone AS, Meek DR, Patil SR. Delays in diagnosis are associated with poorer outcomes in adult hip dysplasia. Scott Med J 2017;62:96–100.
[6] Li Y, Zhang X, Wang Q, Peng X, Wang Q, Jiang Y, et al. Equalisation of leg lengths in total hip arthroplasty for patients with Crowe type-IV developmental dysplasia of the hip: classification and management. Bone Joint Lett J 2017;99-b:872–9.
[7] Canham CD, Yen YM, Giordano BD. Does femoroacetabular impingement cause hip instability? A systematic review. Arthroscopy 2016;32:203–8.
[8] Chen Y, Hu Y, Yu YE, Zhang X, Watts T, Zhou B, et al. Subchondral trabecular rod loss and plate thickening in the development of osteoarthritis. J Bone Miner Res 2018;33:316–27.
[9] Roman-Blas JA, Castaneda S, Largo R, Lems WF, Herrero-Beaumont G. An OA phenotype may obtain major benefit from bone-acting agents. Semin Arthritis Rheum 2014;43:421–8.
[10] Chen L, Hong G, Fang B, Zhou G, Han X, Guan T, et al. Predicting the collapse of the femoral head due to osteonecrosis: from basic methods to application prospects. J Orthop Translat 2017;11:62–72.
[11] Liu XS, Sajda P, Saha PK, Wehrli FW, Guo XE. Quantification of the roles of trabecular microarchitecture and trabecular type in determining the elastic modulus of human trabecular bone. J Bone Miner Res 2006;21:1608–17.
[12] Liu XS, Cohen A, Shane E, Stein E, Rogers H, Kokolus SL, et al. Individual trabeculae segmentation (ITS)-based morphological analysis of high-resolution peripheral quantitative computed tomography images detects abnormal trabecular plate and rod microarchitecture in premenopausal women with idiopathic osteoporosis. J Bone Miner Res 2010;25:1496–505.
[13] Fernandez-Avila DG, Ruiz AJ, Gil F, Mora SA, Tobar C, Gutierrez JM, et al. The effect of an educational intervention, based on clinical simulation, on the diagnosis of rheumatoid arthritis and osteoarthritis. Musculoskelet Care 2018;16:147–51.
[14] Yu YE, Wang J, Zhou B, Edward Guo X. Tissue mineral density dependent mechanical properties of individual trabecula plates and rods do not differ in anatomic directions but individual trabecular directions. J Orthop Transl 2014;2:225–6.
[15] Singh M, Nagrath AR, Maini PS. Changes in trabecular pattern of the upper end of the femur as an index of osteoporosis. J Bone Joint Surg Am 1970;52:457–67.
[16] Fazzalari NL, Parkinson IH. Femoral trabecular bone of osteoarthritic and normal subjects in an age and sex matched group. Osteoarthr Cartil 1998;6:377–82.

[17] Perilli E, Baleani M, Ohman C, Baruffaldi F, Viceconti M. Structural parameters and mechanical strength of cancellous bone in the femoral head in osteoarthritis do not depend on age. Bone 2007;41:760–8.
[18] Liu XS, Sajda P, Saha PK, Wehrli FW, Bevill G, Keaveny TM, et al. Complete volumetric decomposition of individual trabecular plates and rods and its morphological correlations with anisotropic elastic moduli in human trabecular bone. J Bone Miner Res 2008;23:223–35.
[19] Macneil JA, Boyd SK. Bone strength at the distal radius can be estimated from high-resolution peripheral quantitative computed tomography and the finite element method. Bone 2008;42:1203–13.
[20] Van Rietbergen B, Odgaard A, Kabel J, Huiskes R. Direct mechanics assessment of elastic symmetries and properties of trabecular bone architecture. J Biomech 1996; 29:1653–7.
[21] Pritzker KP, Gay S, Jimenez SA, Ostergaard K, Pelletier JP, Revell PA, et al. Osteoarthritis cartilage histopathology: grading and staging. Osteoarthr Cartil 2006; 14:13–29.
[22] Liu XS, Bevill G, Keaveny TM, Sajda P, Guo XE. Micromechanical analyses of vertebral trabecular bone based on individual trabeculae segmentation of plates and rods. J Biomech 2009;42:249–56.
[23] Cohen A, Liu XS, Stein EM, McMahon DJ, Rogers HF, Lemaster J, et al. Bone microarchitecture and stiffness in premenopausal women with idiopathic osteoporosis. J Clin Endocrinol Metab 2009;94:4351–60.
[24] Wehrli FW, Gomberg BR, Saha PK, Song HK, Hwang SN, Snyder PJ. Digital topological analysis of in vivo magnetic resonance microimages of trabecular bone reveals structural implications of osteoporosis. J Bone Miner Res 2001;16:1520–31.
[25] Fu M, Liu J, Huang G, Huang Z, Zhang Z, Wu P, et al. Impaired ossification coupled with accelerated cartilage degeneration in developmental dysplasia of the hip: evidences from muCT arthrography in a rat model. BMC Muscoskelet Disord 2014; 15:339.
[26] Kroker A, Bhatla JL, Emery CA, Manske SL, Boyd SK. Subchondral bone microarchitecture in ACL reconstructed knees of young women: a comparison with contralateral and uninjured control knees. Bone 2018;111:1–8.
[27] Sueyoshi T, Ritter MA, Davis KE, Loder RT. Seasonal variation in adult hip disease secondary to osteoarthritis and developmental dysplasia of the hip. World J Orthop 2016;7:821–5.
[28] Chen Y, Huang YC, Yan CH, Chiu KY, Wei Q, Zhao J, et al. Abnormal subchondral bone remodeling and its association with articular cartilage degradation in knees of type 2 diabetes patients. Bone Res 2017;5:17034.
[29] Li G, Zheng Q, Landao-Bassonga E, Cheng TS, Pavlos NJ, Ma Y, et al. Influence of age and gender on microarchitecture and bone remodeling in subchondral bone of the osteoarthritic femoral head. Bone 2015;77:91–7.
[30] Zhang ZM, Li ZC, Jiang LS, Jiang SD, Dai LY. Micro-CT and mechanical evaluation of subchondral trabecular bone structure between postmenopausal women with osteoarthritis and osteoporosis. Osteoporos Int 2010;21:1383–90.
[31] Kishta W, Abduljabbar FH, Gdalevitch M, Rauch F, Hamdy R, Fassier F. Hip dysplasia in children with osteogenesis imperfecta: association with collagen type I C-propeptide mutations. J Pediatr Orthop 2017;37:479–83.
[32] Wang J, Zhou B, Liu XS, Fields AJ, Sanyal A, Shi X, et al. Trabecular plates and rods determine elastic modulus and yield strength of human trabecular bone. Bone 2015; 72:71–80.
[33] Ding M, Hvid I. Quantification of age-related changes in the structure model type and trabecular thickness of human tibial cancellous bone. Bone 2000;26:291–5.
[34] Laib A, Kumer JL, Majumdar S, Lane NE. The temporal changes of trabecular architecture in ovariectomized rats assessed by MicroCT. Osteoporos Int 2001;12: 936–41.
[35] Zhen G, Wen C, Jia X, Li Y, Crane JL, Mears SC, et al. Inhibition of TGF-beta signaling in mesenchymal stem cells of subchondral bone attenuates osteoarthritis. Nat Med 2013;19:704–12.
[36] Shi X, Liu XS, Wang X, Guo XE, Niebur GL. Effects of trabecular type and orientation on microdamage susceptibility in trabecular bone. Bone 2010;46:1260–6.
[37] Sepriano A, Roman-Blas JA, Little RD, Pimentel-Santos F, Arribas JM, Largo R, et al. DXA in the assessment of subchondral bone mineral density in knee osteoarthritis–A semi-standardized protocol after systematic review. Semin Arthritis Rheum 2015; 45:275–83.
[38] Kroker A, Zhu Y, Manske SL, Barber R, Mohtadi N, Boyd SK. Quantitative in vivo assessment of bone microarchitecture in the human knee using HR-pQCT. Bone 2017;97:43–8.
[39] Liu XS, Zhang XH, Sekhon KK, Adams MF, McMahon DJ, Bilezikian JP, et al. High-resolution peripheral quantitative computed tomography can assess microstructural and mechanical properties of human distal tibial bone. J Bone Miner Res 2010;25: 746–56.